Available online at www.sciencedirect.com
SCIENCE DIRECT
International Journal of Fatigue 27 (2005) 991–1005
International Journal of Fatigue
www.elsevier.com/locate/ijfatigue

# What is fatigue damage? A view point from the observation of low cycle fatigue process

Y. Murakami[a,*], K.J. Miller[b]

[a]Department of Mechanical Engineering Science, Kyushu University, 6-10-1 Hakozakiv, Hakozaki-ku, Fukuoka 812-8581, Japan
[b]Department of Mechanical Engineering, SIRIUS, University of Sheffield, Sheffield S1 3JD, UK

Received 21 July 2004; received in revised form 27 September 2004; accepted 18 October 2004

**Abstract**

Fatigue damage requires to be expressed in terms of a crack. This will be revealed by several items of experimental evidence. First, observations on a medium carbon steel that relate to the initiation zones and the propagation of small cracks subjected to low cycle fatigue, will be presented; these observations being based on surface replica studies. It will be shown that the Coffin-Manson high-strain, low-cycle, fatigue relationship is substantially the same as a crack growth law. Second, the effect of prior fatigue history on the growth rate of a small crack is investigated systematically using special specimens containing an artificial small hole of various diameters, i.e. 40, 100 and 200 μm. Prior fatigue history is shown to have little influence on the crack growth rate in the high-strain fatigue regime. Third, it will be revealed that the loss of fracture ductility after strain cycling in high-strain fatigue tests is attributable to the existence of small surface cracks. The loss of fracture ductility depends on the crack length $l$. If $l$ is larger than a critical length $l$(c), the fatigue crack causes macroscopic shear fracture in a tensile test following strain cycling. On the other hand, if $l$ is smaller than $l$(c), the tensile fracture surfaces are of the cup-and-cone type. For 70/30 brass, $l$(c) is about 400 μm. Thus, fatigue damage models which ignore the reality of fatigue damage as expressed in terms of cracks should not be used for fatigue life predictions.


*Keywords:* Fatigue damage; Low cycle fatigue; Small crack; Ductility; The Coffin-Manson low

## 1. Introduction

What is fatigue damage? How, when and where is it accumulated? Can damage be quantified with accuracy, especially for realistic loading conditions that apply to components and structures, made from a wide variety of engineering materials?

These critical questions have been explored for more than a century and yet misleading paths, together with misconceptions about the nature of fatigue, and finally false conclusions abound in the literature. These aspects require to be eliminated if progress in our under-standing of fatigue damage accumulation is to be made.

This paper presents a quantifiable and physically realistic answer to the question: 'What is Fatigue Damage? ' from the viewpoint of low cycle fatigue.

In an attempt to remove uncertainties and misconceptions, it is necessary to turn to experimental evidence and to quantify that evidence in an unambiguous manner. Hopefully such an endeavour will assist more rapid progress to be made on the problem of assessing damage accumulation.

In this paper, we examine the low-cycle fatigue regime under push–pull (axial) loading conditions which is mainly concerned with tensile-type cracking (i.e. Stage II cracks) and where Stage I (shear type) cracks are confined to a depth of only one or two surface grains [1]. However, the results presented here can also be applicable to dominant shear (i.e. Stage I) cracks generated under torsion loading.

Two quite different types of investigation have historically been conducted in the low-cycle fatigue regime, one led by Coffin [2] and Manson [3] relating to a cyclic deformation approach, and the second by Tomkins [4] and others, e.g. Boettner et al. [5], Liu [6] and Frost [7] relating

* Corresponding author. Tel.: +81 92 642 3380; fax: +81 92 641 9744.
*E-mail address:* ymura@mech.kyushu-u.ac.jp (Y. Murakami).

0142-1123/$ - see front matter © 2005 Elsevier Ltd. All rights reserved.
doi:10.1016/j.ijfatigue.2004.10.009

to a cyclic fracture approach. Tomkins provided a comprehensive analytical model as well as experimental data. This present paper, however, will show experimentally and theoretically, that both types of investigation are complementary to one another, i.e. a fatigue crack growth approach leads directly to the Coffin-Manson relationship given by

$$\Delta\varepsilon_p N_f^{\alpha} = C_1 \tag{1}$$

where $\Delta\varepsilon_p$ is the cyclic plastic strain range, $N_f$ is the number of cycles to failure, and $C_1$ and $\alpha$ are material constants. The exponent $\alpha$ usually varies from 0.5 to 0.7 [8], and is dependent on whether torsion or axial loading is being investigated. Unfortunately, the gradual but steady accumulation of damage, cycle-by-cycle, is not quantifiable by the Coffin-Manson approach, only the terminal condition of final fracture. Different lifetimes can be obtained at a constant stress or strain range, should the strain rate change (either in a regular or irregular manner) throughout a test, particularly if hold times are introduced at maximum stress or strain in a cycle. Consequently it is essential to know what processes and mechanisms are involved from the first application of a cyclic load, all the way through to the final load application that causes complete fracture.

Tomkins examined the growth of artificially induced *macro* edge cracks in various materials subjected to low-cycle fatigue conditions, and presented a crack growth rate ($da/dN$) equation of the form

$$da/dN = C_2 \Delta\varepsilon_p^n a \tag{2}$$

where $C_2$ and $n$ are material constants. However, the initial period of lifetime, which is associated with the creation and growth of *micro*-cracks, will be shown to be an important period in the fatigue lifetime of smooth surface samples [9,10]. This paper concentrates on the important period of fatigue lifetime when assessing the true meaning of fatigue damage and hence the elimination of the previously stated mis-conceptions.

## 2. Fatigue damage in low-cycle fatigue and the behaviour of small cracks

### 2.1. Material and test procedure

The material used was a carbon steel round bar; type S45C (0.46% C, diameter 22 mm)[11]. The material was first annealed at 844 °C for an hour, and then machine-turned. The chemical composition and mechanical properties of this material are given in Table 1. The mean ferrite grain size is about 19 μm and the mean pearlite grain size is about 17 μm. Hour-glass shaped specimens, see Fig. 1(a), having a minimum diameter of 8 mm at the central cross-section, and a stress concentration factor of 1.027, were used in the fatigue tests. The specimen surface was finished with emery paper (Grade No. 06), and then about 30 μm on the specimen diameter was removed by electro-polishing. These specimens are called 'plain specimens'. To simulate a defect or an inclusion, a very small hole was drilled on the periphery of the central portion of a plain specimen. The diameter $d$ of the hole and its depth were identical, as indicated in Fig. 1(b). Three hole diameters were used, with $d$ equal to 40, 100 or 200 μm. These specimens are called 'holed specimens'.

Table 1
Chemical composition and mechanical properties[a]

| Chemical composition (wt %) | | | | Mechanical properties | | | |
|---|---|---|---|---|---|---|---|
| C | Si | Mn | P | $\sigma_s$ | $\sigma_B$ | $\sigma_T$ | $\psi$ |
| 0.46 | 0.27 | 0.74 | 0.015 | 284 | 543 | 889 | 48.9 |
| S | Cu | Ni | Cr | | | | |
| 0.02 | 0.02 | 0.01 | 0.10 | | | | |

$\sigma_B$, Ult. tensile strength (MPa); $\sigma_T$, true fracture stress (MPa); $\psi$, reduction of area (%).
[a] $\sigma_s$, yield stress (MPa).

Push–pull low-cycle fatigue tests were carried out on a closed-loop, electro-hydraulic servo-controlled testing machine that kept the cyclic stress amplitude constant. The test frequency was in the range 0.06–0.6 Hz, depending on the particular stress–strain range; a lower test frequency was used at the higher strain ranges in order to avoid heating of a specimen. The cyclic stress–strain property was obtained as:

$$\Delta\sigma/2 = 1.23 \times 10^3 \Delta\varepsilon_p^{0.26} \tag{3}$$

Continual observations of microcrack initiation zones and surface crack growth in the various specimens were recorded either by an optical microscope or a plastic replica technique.

### 2.2. Experimental results and discussion

#### 2.2.1. Fatigue failure lives of plain and holed specimens

Fatigue failure lives $N_{f0}$ and $N_f$ of plain and holed specimens were obtained at five different load levels equivalent to cyclic stress levels in the range from $\pm 294$ to $\pm 530$ MPa. Fig. 2 shows the log–log relation between the cyclic plastic strain range $\Delta\varepsilon_p$ and the number of stress cycles to failure $N_{f0}$ and $N_f$ of the specimens. The figure indicates that (i) the $\Delta\varepsilon_p - N_f$ relations of both plain and holed specimens show linear relationships of the Coffin-Manson type, (ii) slopes of the log–log relations of each specimen type are similar, and (iii) the fatigue life decreases with an increase in the diameter of hole $d$. In all cases, $N_f$ was defined by the instant when complete separation of the gauge length occurred, i.e. when the observed surface propagating crack had propagated sufficiently through the thickness to cause rupture of the remaining cross-sectional area. The similar slopes of all four curves of Fig. 2, is indicative of the same fatigue process being operative

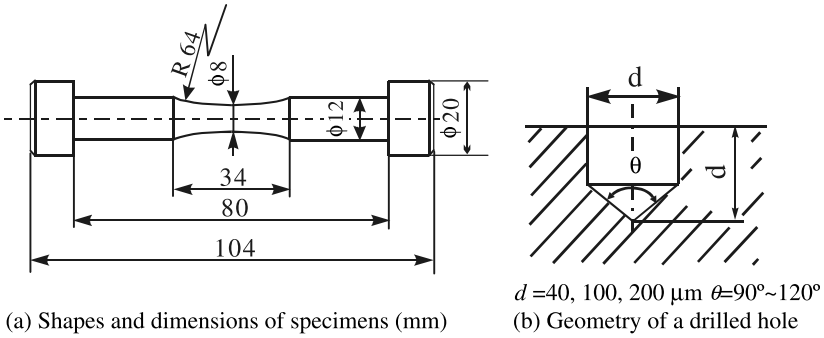


Fig. 1. Shapes and dimensions of specimens and geometry of a drilled hole.

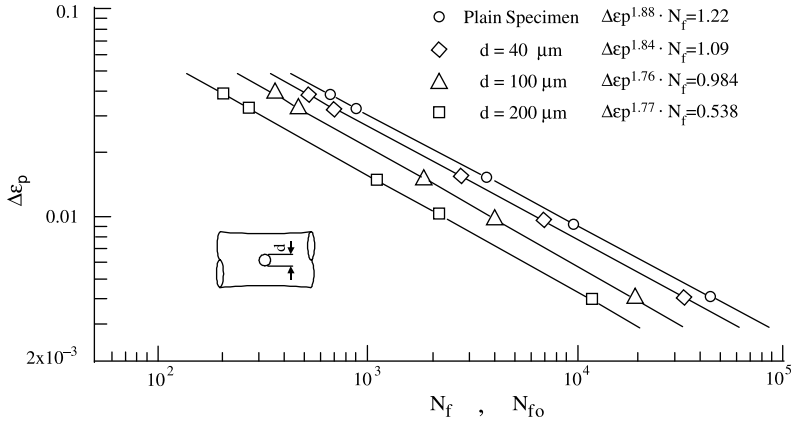


Fig. 2. Relationship between cyclic plastic strain range ($\Delta\varepsilon_p$) and the number of cycles to failure of plain and holed specimens.

(i.e. Stage II crack growth) in all specimens, irrespective of the applied cyclic stress–strain level.

Fig. 3 shows the initiation and growth behaviour of a crack emanating from holes with different diameters, while Fig. 4 indicates the correlation between the dimensionless fatigue life $N_f/N_{f0}$ and the diameter $d$ of the initial hole of specimens at each load level. The experiments show a trend whereby the fatigue life $N_f/N_{f0}$ becomes longer with decreasing $d$. In the case of the specimen with the smallest hole diameter ($d=40$ μm), the fatigue life is about the same as that of plain specimens. This can be appreciated should the residual life-time of plain specimens containing microcracks of about 10–20 μm long be plotted on Fig. 4 for comparative purposes. This residual lifetime is greater than 0.9. Judging from the observed trends in Fig. 4, we can say that the total fatigue life of plain specimens is dominated by crack propagation, i.e. the Coffin-Manson relation virtually represents a crack propagation law.

### 2.2.2. Crack propagation life of plain and holed specimens

Fig. 5 indicates a dimensionless, so-called by some investigators the 'crack initiation' life $N_C/N_f$ and the crack propagation life $N_{1\ mm}/N_f$ of specimens. Here $N_C$ is the number of cycles at which a propagating surface crack is first observed, which is increasingly difficult to assess the lower the stress–strain range, while $N_{1\ mm}$ is the number of

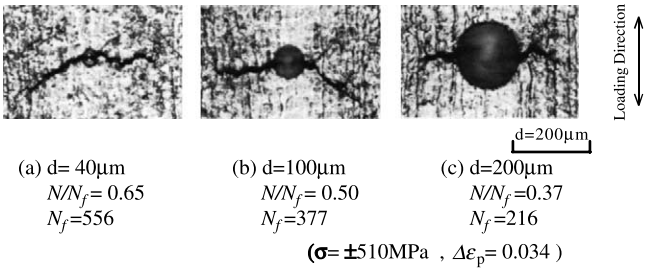


Fig. 3. Crack propagation from artificial drilled holes, $\Delta\sigma=\pm510$ MPa, $\Delta\varepsilon_p=0.034$.

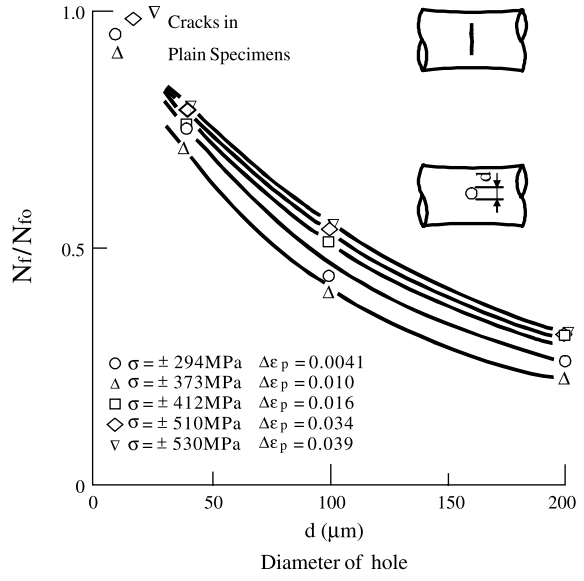


Fig. 4. Dimensionless fatigue lives of holed specimens defined by relative life to plain specimen. $N_{f0}$, Fatigue life of plain specimen, $N_f$, fatigue life.

cycles for the surface crack to reach 1 mm in length. Finally $N_f$ is the total number of cycles to failure. This consequently is a function of the depth of a crack, and hence the depth of the hole. The value $N_C/N_f$ is at most about 0.08 at the lowest stress level tested, and it becomes smaller than 0.02 at a higher load level where $N_f < 10^4$. Therefore, the total life of specimens is dominated by crack propagation. The crack initiation site in holed specimens was always either at the surface edge, or at the root of the hole.

Using the plastic replica technique, the initiation and propagation of a dominant surface crack were continuously observed on plain specimens. The results in Fig. 6 reveal that the dominant crack has already initiated within the first early stress cycles. In an extreme case, crack initiation was detectable during the very first tensile stress cycle. In order to check this point in detail, a static tensile test of a plain

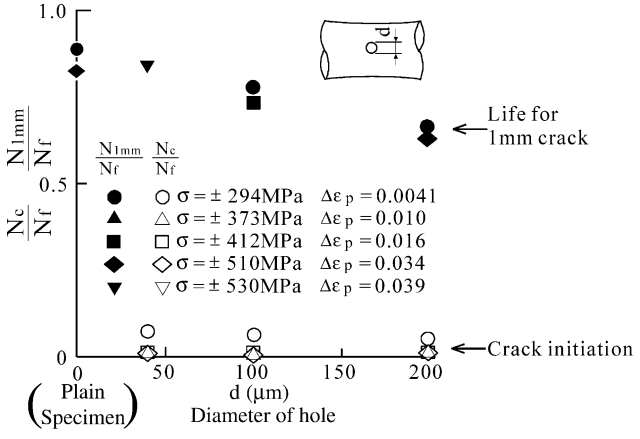


Fig. 5. Dimensionless crack initiation lives and fatigue lives at which a microcrack grew to 1-mm long in holed specimens. $N_c$ is defined by the cycle at which a cycle appeared at the edge of the hole.

specimen was conducted. By interrupting the loading at different points of the tension cycle, microcrack initiation on the specimen surface was observed. Such microcracks are illustrated in Fig. 7. The microcrack initiation sites were located either in pearlite grains or in a ferrite matrix between two adjacent pearlite zones. Fig. 8 shows the relationship between tensile stress and crack density.

Summarising, it can be stated with sufficient accuracy that the push–pull low-cycle fatigue process is substantially identical to the Stage II crack growth process. The importance of the crack growth process in relation to the crack initiation process when considering low-cycle fatigue behaviour has been pointed out in several previous studies. However, due to a lack of detailed information on microcrack initiation and propagation in the low-cycle fatigue regime, confusion and ambiguity still exist concerning the 'crack initiation' life. This has been arbitrarily defined by engineers and researchers for many years by invoking a crack length that has already propagated a small distance. It is not surprising, therefore, that it has previously been reported that the crack initiation life satisfies a relation of the Coffin-Manson type, even if a different crack length was used in defining the crack initiation life. This fact confirms that the Coffin-Manson relation is an alternative expression for a crack propagation law [11–13]. Hence, the so-called 'crack initiation' life defined by the initiation of an 'engineering-size crack' (i.e. easily observable) is substantially the number of cycles required from the time of initiating a surface imperfection or a grain-size crack to the time of the formation of a not inconsiderable length of crack. In the present study, the number of stress cycles required to form a grain-size crack is negligibly small in the low-cycle fatigue regime. To avoid uncertainty associated with the definition of a crack initiation life in an engineering sense, it could perhaps be defined as the cycles of fatigue crack propagation required for a microcrack to grow to an easily definable length such as 0.5 or 1 mm in length. Alternatively, $N_C$ can unambiguously be regarded as of zero duration, certainly within the low-cycle fatigue regime. This alternative eliminates any possible confusion.

### *2.2.3. Relationship between the microcrack propagation law and the Coffin-Manson expression*

The size of the propagating microcrack is very small when compared with the size of a representative specimen or component. Therefore, no significant change in the applied constant cyclic strain amplitude in the bulk material occurs during microcrack growth, hence the Coffin-Manson relation is expected to be related to, and correlated with, the crack propagation law. Fig. 9(a)–(d) show the relationship between the surface crack length $l$ and the dimensionless number of cycles $N/N_f$ at each stress amplitude for both plain and holed specimens. In order to correlate the crack growth rate d$l$/d$N$ with the crack length $l$ for each specimen, the relation of the crack growth rate vs the applied stress amplitude was first determined. From the results of the crack

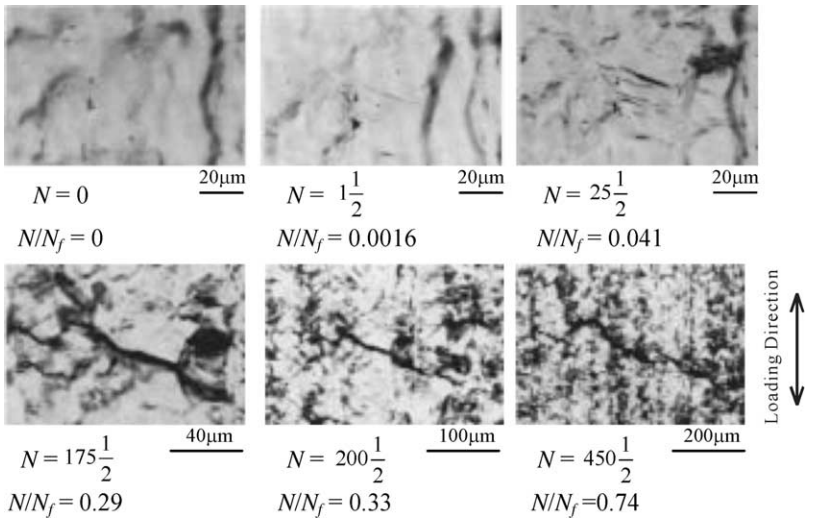


Fig. 6. Microcrack initiation and propagation continuously observed on the plain specimen.

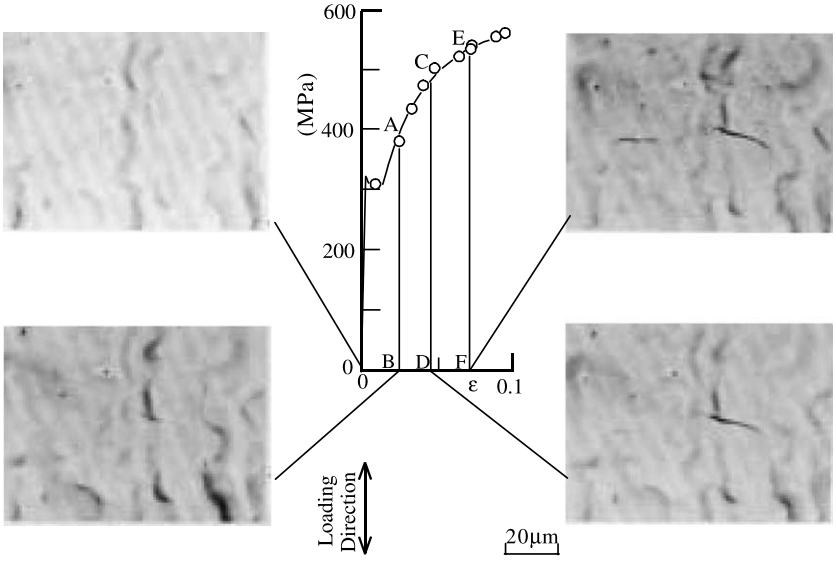


Fig. 7. Crack initiation during the first tensile process of a plain specimen.

growth rate for the same crack length under different stress amplitudes, the following equations were derived using the data of Fig. 9. First

$$dl/dN = (\Delta\sigma/2)^{6.7} f(l) \quad (\Delta\sigma \text{ in MPa and } l \text{ in } \mu\text{m}) \tag{4}$$

where *f(l)* implies a function of *l*. For the holed specimens, the valid crack growth data were employed after a microcrack had grown to a length three times as long as the diameter of the initial hole. Moreover, to obtain the d*l*/d*N* versus *l* relation, the quantity $(dl/dN)/(\Delta\sigma/2)^{6.7}$ was plotted against *l*, as indicated in Fig. 10. Evidently the relation satisfies a linear form on the log–log diagram, although the plotted data is scattered to some extent.

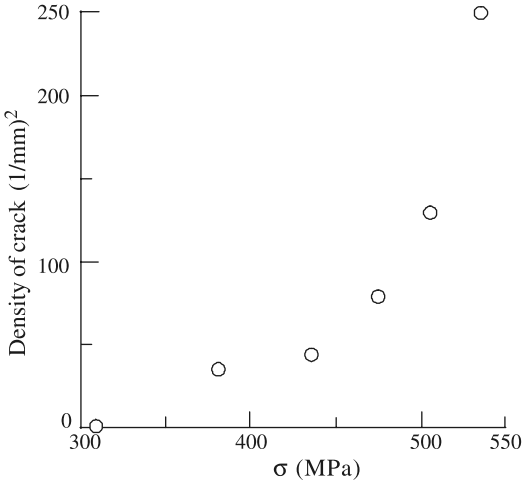


Fig. 8. Density of microcracks in a static tensile test of a plain specimen.

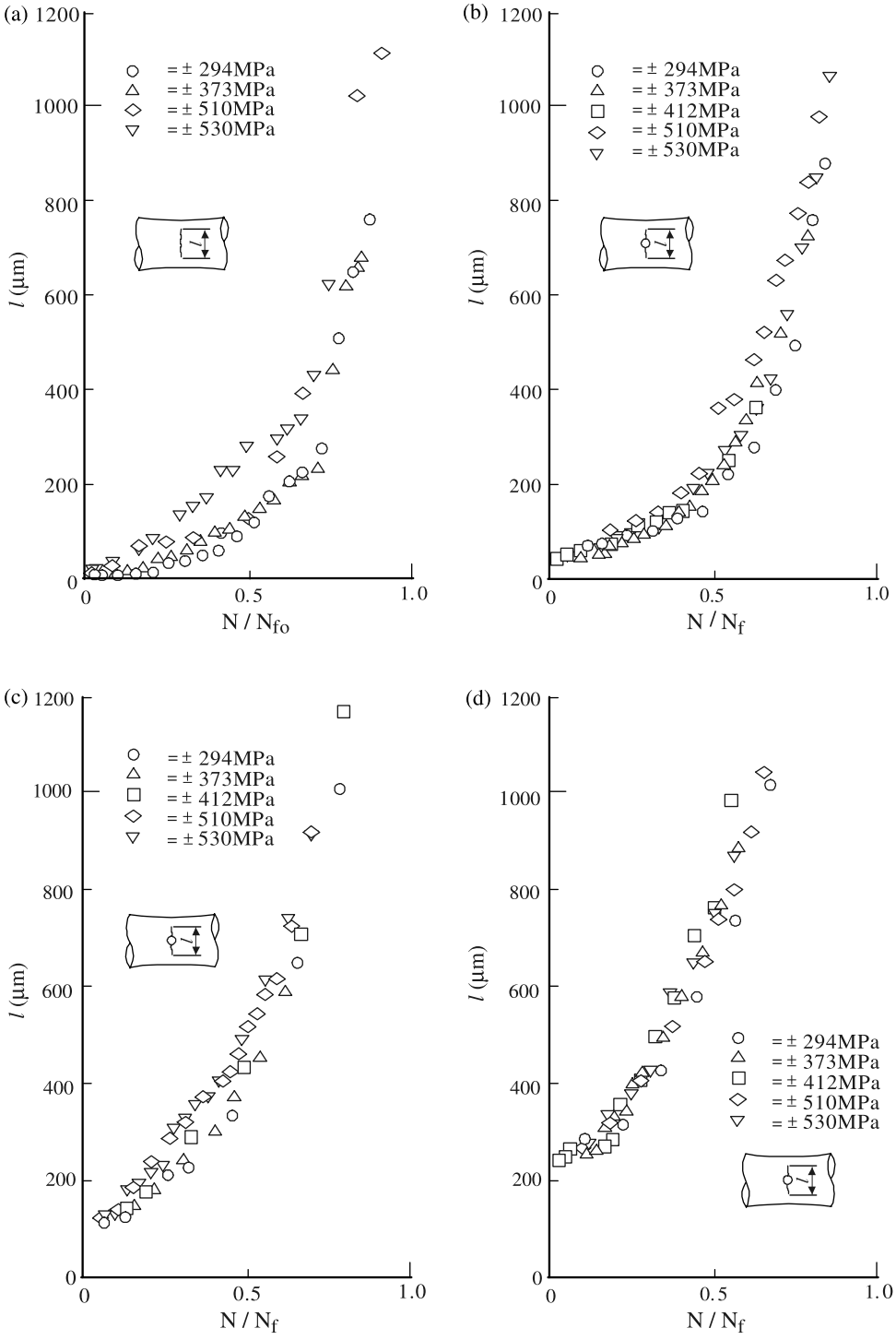


Fig. 9. Crack propagation curves: (a) plain specimen, (b) $d=40$ μm, (c) $d=100$ μm and (d) $d=200$ μm.

The following equation is obtained from the results (Fig. 11)

$$dl/dN = 5.12\times10^{-21}(\Delta\sigma/2)^{6.7}l \quad (\Delta\sigma \text{ in MPa and } l \text{ in } \mu\text{m}) \tag{5}$$

In order to derive the Coffin-Manson relation, Eq. (1), from the crack propagation law, Eq. (5), we first integrate Eq. (5) to obtain

$$\ln(l_f/l_0) = 5.12\times10^{-21}(\Delta\sigma/2)^{6.7}(N_f - N_0) \tag{6}$$

where $l_0$ represents the initial surface crack length at the number of stress cycles $N_0$, and $l_f$ is the final crack length at failure ($N=N_f$). Eq. (6) coincides with that proposed by

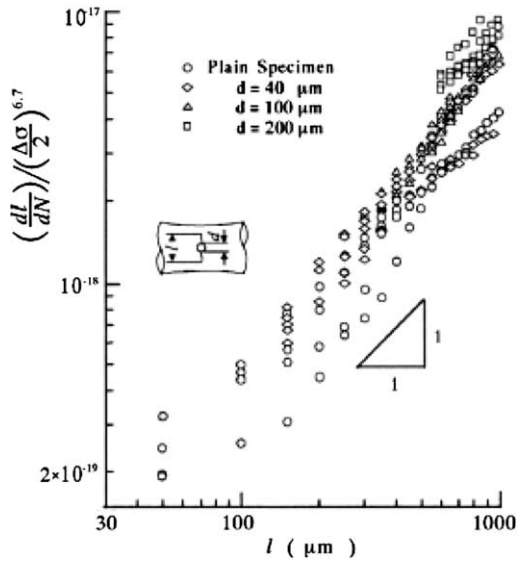


Fig. 10. Relation between crack length and crack growth rate.

Weiss [14]. Substituting the following approximate conditions into Eq. (6):

$l_0$ the size of a pearlite grain (=17 μm) or the diameter $d$ of the holed specimens (40, 100 or 200 μm)
$l_f$ the minimum diameter of the specimen (=8 mm)
$N_0$ 0 (since $N_0 \ll N_f$).

then for a plain specimen:

$$(\Delta\sigma/2)^{6.7} N_f = 1.20 \times 10^{21} \text{ or } \Delta\varepsilon_p N_f^{0.575} = 1.65 \quad (7)$$

and for holed specimens:

$$(\Delta\sigma/2)^{6.7} N_f = 1.03 \times 10^{21} \text{ or } \Delta\varepsilon_p N^p = 1.51 \quad (\text{when } d = 40\ \mu\text{m}) \quad (8)$$

$$(\Delta\sigma/2)^{6.7} N_f = 8.56 \times 10^{20} \text{ or } \Delta\varepsilon_p N^p = 1.36 \quad (\text{when } d = 100\ \mu\text{m}) \quad (9)$$

$$(\Delta\sigma/2)^{6.7} N_f = 7.20 \times 10^{20} \text{ or } \Delta\varepsilon_p N^p = 1.23 \quad (\text{when } d = 200\ \mu\text{m}) \quad (10)$$

(i) the larger and deeper holes, in comparison to plain and 40-μm hole specimens, which will influence the through-thickness crack growth rate, and hence a final failure condition which will occur sooner, and
(ii) in plain (and probably the very small 40-μm surface hole) specimens the first crack growth phase over the first one or two grains will be for the slower Stage I (shear) cracks which are not inclined in the same direction as the subsequent Stage II cracks.

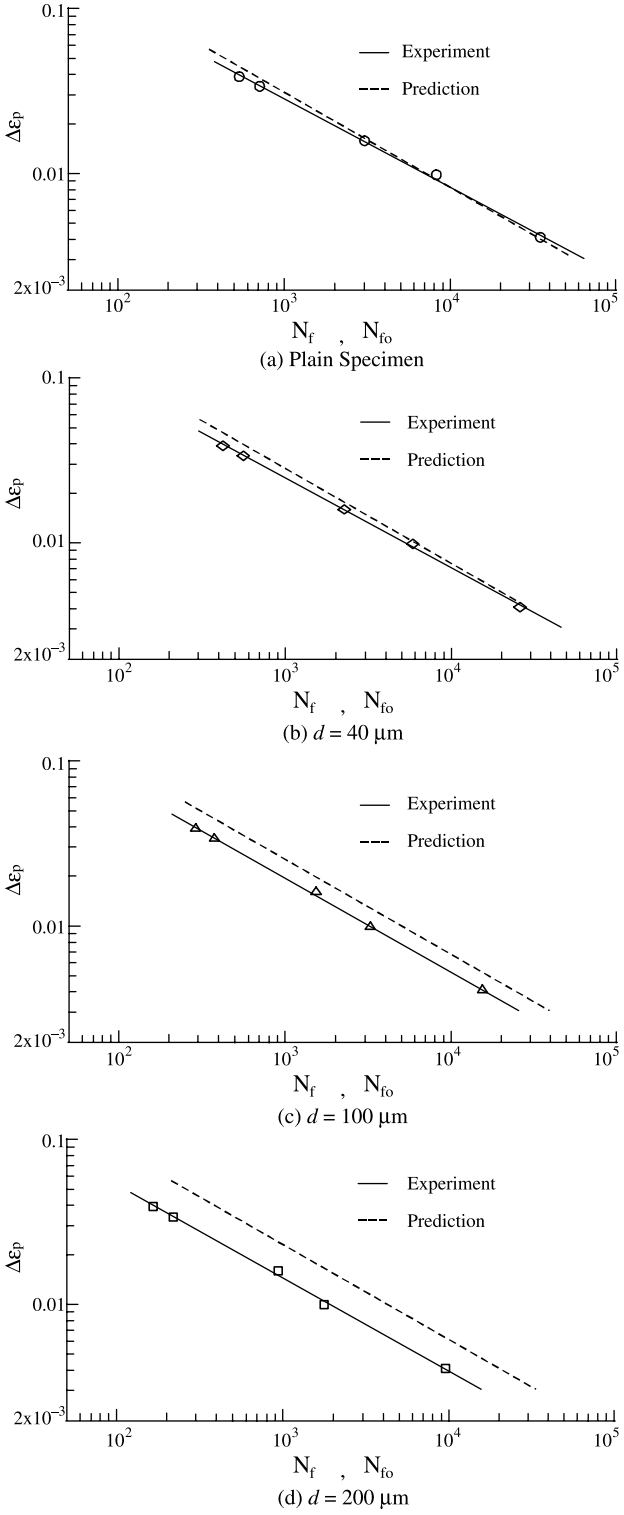


Fig. 11. Comparison of experimentally determined fatigue lives and predictions by Eqs. (7)–(10).

In the case of the specimen with the smallest hole diameter and depth, $d$=40 μm, this size is almost equal to only two grain sizes of the test material. The error in prediction becomes very small in such a case. It should also be remembered that in smooth plain specimens subjected to

low-cycle fatigue conditions, several cracks will form, and hence the formation of a dominant Stage II crack will be a little delayed.

### 2.2.4. Effect of prior cyclic stress or strain history on subsequent crack growth rate

Here we consider zones of material ahead of a crack tip which, from one historical viewpoint, accumulates damage per cycle as lifetime progresses. To examine this possibility, Fig. 12 indicates material in the cross-hatched zones that could be accumulating damage ahead of a crack of length $l^*$, here chosen to be 400 μm. By choosing holes of different initial diameters (40, 100 and 200 μm) the material ahead of the surface crack tip would have accumulated different extents of damage because the material elements would have sustained very different numbers of fatigue cycles prior to the crack attaining the length $l^*$ especially when compared with the plain specimen.

Fig. 13 plots the crack propagation life for a crack to attain 400 μm in length (the abscissa) which is approximately 0.7 of the lifetime for a plain specimen and only approximately 0.08 of the lifetime for the largest hole specimen. Despite this very large difference in accumulated cycles within the zone ahead of the crack, there is very little difference in the residual fatigue life as the surface crack propagates from 0.4 mm to the failure length, irrespective of the cyclic stress level applied.

This fact indicates that the prior fatigue history within the zone where the crack has not yet propagated during the period of crack growth up to 400 μm in length, has no effect on the subsequent crack growth rate. The same result is obtained when the reference crack length $l$ is changed. These results lead to an important conclusion, namely that prior fatigue history hardly influences the subsequent microcrack growth rate in the low-cycle fatigue range.

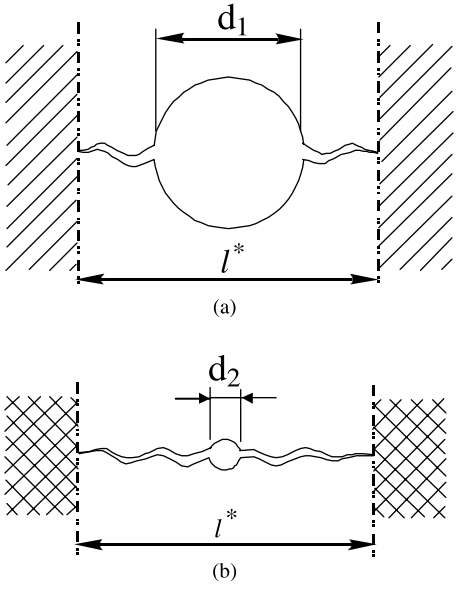


Fig. 12. Prior fatigue region for two holed specimens with a different diameter of the initial hole and with the same crack length (a) specimen with a large hole, (b) specimen with a small hole.

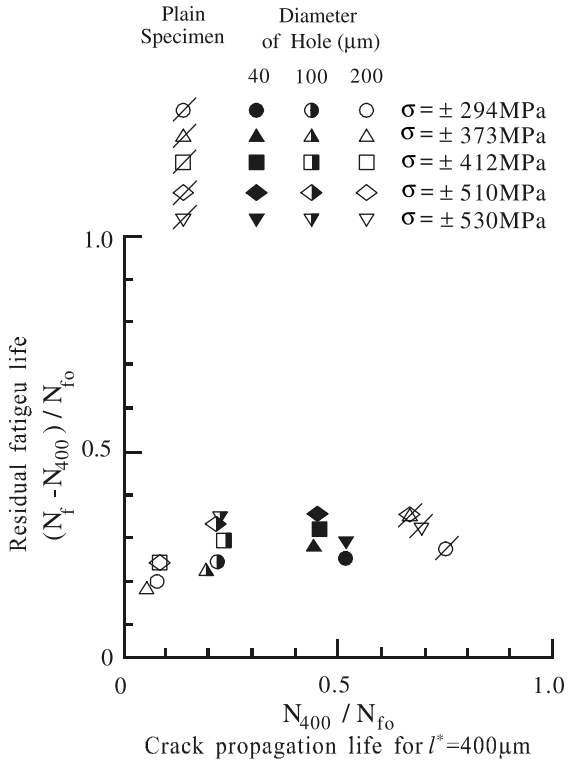


Fig. 13. Residual fatigue life holed specimens after a microcrack grows to 400-μm long.

### 2.2.5. The applicability of the Palmgren-Miner cumulative damage rule

It has been reported by many investigators that the Palmgren-Miner (P-M) rule [15,16] is often satisfied for various kinds of materials. The P-M rule states:

$$\sum \frac{n}{N_f} = \frac{n_1}{N_{f_1}} + \frac{n_2}{N_{f_2}} + \cdots = 1.0 \tag{11}$$

when $n_1$ is the number of cycles at the stress or strain range level 1, and $N_{f1}$ is the number of cycles to failure at that stress or strain range, etc.

When estimating fatigue damage under complex variable loading conditions the concept of the P-M rule is frequently invoked along with various damage counting methods [17–19]. Considering the discussion given in the preceding section, the P-M rule should now be assessed on the basis of the microcrack propagation law. Consequently, fatigue crack propagation tests were performed on a specimen with $d = 40$ μm under a two-level loading condition. The results are shown in Table 2. The initial cyclic stress amplitude was switched when a microcrack grew to about 200 μm in length. Recalling the fact that the initial small hole can be regarded as an initial crack of identical length, it is evident from Table 2 that the P-M rule is satisfied according to microcrack growth mechanics. In previous

Table 2
Fatigue damage accumulation under two-level loading

| $\sigma_1$ (MPa) ($\Delta\varepsilon_{pl}$) | $\sigma_2$ (MPa) ($\Delta\varepsilon_{p2}$) | $(n_1/N_{f1})$ | $(n_2/N_{f2})$ | $\sum(n_i/N_{fi})$ |
|---|---|---|---|---|
| ±294(0.0041) | ±530(0.039) | 0.55 | 0.67 | 1.22 |
| ±530(0.039) | ±294(0.0041) | 0.58 | 0.54 | 1.12 |
| ±530(0.039) | ±373(0.010) | 0.48 | 0.67 | 1.15 |

work [14,20] the P-M rule has also been derived on the basis of crack propagation behaviour. The required conditions for satisfying the P-M rule are:

1. prior fatigue history has no effect on the subsequent crack growth rate.
2. crack growth rate is linearly proportional to crack length.
3. The crack growth process is the same at all strain range levels, i.e. either a Stage I or a Stage II crack growth process.
4. The final crack length $l_f$ is similar for all strain range levels.
5. The orientation of the applied stress–strain field does not change.

These conditions are introduced in the case of a two-level loading test where $\Delta\varepsilon_{p1}$, is the strain range at the first level for a duration of $n_1$ cycles when the crack grows from $l_0$ to $l_1$, while $\Delta\varepsilon_{p2}$ is the second level for a period of $n_2$ cycles when the crack grows from $l_1$ to $l_2$ (=the failure crack length $l_f$). It follows from any equation of the form given by Eq. (2)—or in stress terms Eq. (5), i.e.

$$dl/dN = D\Delta\varepsilon_p^{\beta} l \quad \text{where } D \text{ is a constant} \tag{12}$$

that

$$\ln(l_f/l_0) = D\Delta\varepsilon_{pl}^{\beta} N_{f1} \tag{13}$$

$$\ln(l_f/l_0) = D\Delta\varepsilon_{p2}^{\beta} N_{f2} \tag{14}$$

$$\ln(l_1/l_0) = D\Delta\varepsilon_{pl}^{\beta} n_1 \tag{15}$$

$$ln(l_2/l_1) = D\Delta\varepsilon_{p2}^{\beta} n_2 \tag{16}$$

Hence,

$$n_1/N_{f1} + n_2/N_{f2} = \ln(l_1/l_0)/\ln(l_f/l_0) + \ln(l_f/l_1)/\ln(l_f/l_0) = 1 \tag{17}$$

Similar considerations can be applicable to multi-level variable loading. The problem of whether the previous equations hold or not has been ignored, or has been regarded as self-evident in several multi-level studies. However, this problem should be verified experimentally whilst recalling the assumptions used when meeting cases where the P-M rule is not applicable. In this respect prior fatigue history can hardly influence subsequent microcrack growth in most materials because:

1. from a macroscopic viewpoint, a steady-state cyclic hysteresis loop is rapidly reached i.e. within a few early stress cycles, even should the cyclic stress amplitude be varied [8,21,22], and
2. from a microscopic viewpoint, a unique saturated dislocation structure appears irrespective of prior history [23].

For a material in which no unique dislocation structure is recovered after variations of stress amplitude [23], different trends might be seen that need to be related to the validity of the P-M rule and the crack propagation law.

## 3. Ductility loss during the fatigue process

### *3.1. Effects of small surface cracks on ductility loss during low cycle fatigue*

For Eq. (1), Coffin [24] proposed that the value of $C_1$ can be correlated with material ductility $\varepsilon_f$ as given by:

$$C_1 = 1/2\varepsilon_f : \text{here } \varepsilon_f = \ln A_0/A = \ln[1/(1-\psi)] \tag{18}$$

The term $A_0$ is the initial area, $A$ is the area of the minimum cross-section after tensile testing, and $\psi$ is reduction of area. The values and the physical meaning of the terms $\alpha$ and C have been examined by many researchers, e.g. [25]. The view that the constant $C_1$ can be correlated with material ductility has been connected with ambiguous concepts of fatigue damage. One historical concept of fatigue damage [26] has been thought to be the weakening or losing of the strength of a material due to irreversible slip in crystals or plastic strain cycling. In fact, it has been experimentally verified that the value of the residual fracture ductility ($\varepsilon_f$) of fatigued specimens is lower than that of the virgin state, and the decrease in fracture ductility becomes predominant as the number of cycles $N$ approaches $N_f$. On the other hand, experiments show that the fracture life ($N_f$) can be extended when the surface layer of a specimen is removed during fatigue testing, though cyclic strain hardening or softening occurs in the bulk material of a specimen [10,20]. These phenomena suggest that in order to identify the real meaning of fatigue damage, we must pay attention to the surface layer condition of a specimen.

In his investigation, Coffin [2] mentioned that the scatter of residual fracture ductility data was quite wide and that this was a result of variations in the occurrence and size of fatigue cracks formed during thermal stress cycling. After Coffin's early work, similar tests were conducted by other researchers and similar conclusions were derived. In their early study, Sessler and Weiss conjectured that fatigue damage must be correlated with both the decrease in strength quality in the bulk of a specimen, and with surface cracks [27]. However, it has been clearly shown that

a change in the surface layer condition of a specimen is more crucial when assessing fatigue damage.

In Section 2 of this paper, it was explained that the low cycle fatigue process is dominated, almost 100%, by crack growth processes and that the Coffin-Manson law is another expression of the growth law of small cracks. On the other hand, we know from experiments that fracture ductility is actually lost during low-cycle fatigue. Therefore, the correlation between fatigue damage and residual fracture ductility must be clarified from the standpoint of the correlation between the existence of small cracks on a specimen surface and ductility loss. Ohtani et al. [28] and Kikukawa et al. [9] indicated that the loss of fracture ductility in low cycle fatigue of a 0.2% carbon steel, is caused not only by surface cracks, but by internal cracks in pearlite grains. However, internal cracking was observed only under large plastic strain ranges, i.e. $\Delta\varepsilon_p > 10\%$. In such cases, it is the triaxial stress state induced in the centre of a specimen that results in internal cracking. Kikykawa et al. [9] and Ohtani et al. [28] also show that for small values of $\Delta\varepsilon_p$ a decrease in fracture ductility was observed only at later states in the fatigue life and only when the crack length was longer than 2 mm. These experimental facts suggest that the fracture ductility for smaller crack lengths, and the ductility of specimens following the removal of the surface layer containing cracks, must be investigated separately in order to reveal the effects of cracks and bulk condition of a specimen.

### 3.2. Material and test procedure

The material used for test specimens was a 70/30 brass in the form of rolled plates (23×220×1275 mm) [29]. The original blocks of the material were annealed at 400 °C for 40 min and then machine-turned. The chemical composition and mechanical properties of this material are shown in Table 3. Hourglass-shaped specimens, having a minimum diameter of 8 mm, were used. These specimens are called 'plain' specimens. Specimens containing a drilled hole on their surface, in the centre portion, were also used. The diameter ($d$) of the hole is the same as its depth ($h$) (Fig. 1(b)), i.e. 200 μm. Both 'plain' and 'holed' specimen surfaces were finished with emery paper (Grade No 06). All specimens were annealed in a vacuum for 40 min at 400 °C and then a surface layer of 20 μm depth was removed by electro-polishing. The small artificial hole was drilled after electro-polishing. Fig. 14 shows the relationship between

Table 3
Chemical composition and mechanical properties[a]

| Chemical composition (wt %) | | | | Mechanical properties | | | |
|---|---|---|---|---|---|---|---|
| Cu | Fe | Pb | Zn | $\sigma_{0.2}$ | $\sigma_B$ | $\sigma_T$ | $\psi$ |
| 70.2 | 0.01 | tr. | bal. | 196 | 340 | 1088 | 79.1 |

$\sigma_T$, true fracture stress (MPa); $\sigma_B$, tensile strength (MPa); $\psi$, reduction of area (%).
[a] $\sigma_{0.2}$, 0.2% proof stress (MPa).

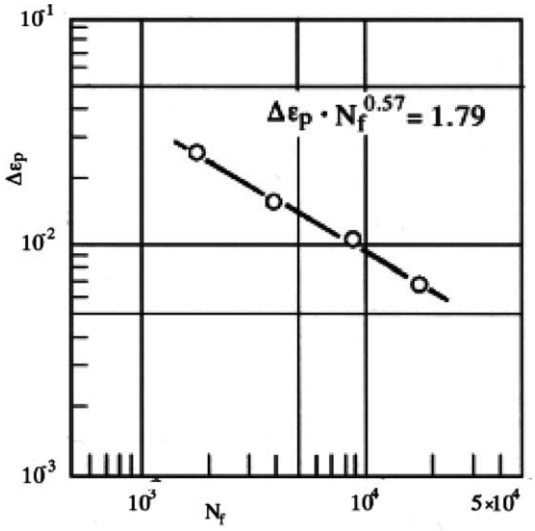


Fig. 14. Relationship between cyclic plastic strain range ($\Delta\varepsilon_p$) and number of cycles to failure ($N_f$) of plain specimens.

the cyclic plastic strain range ($\Delta\varepsilon_p$) and the number of cycles to failure ($N_f$) during the stress-controlled low-cycle fatigue tests. The values of true maximum tensile stress and true maximum compressive stress were kept equal throughout a test.

Another series of strain-controlled low-cycle fatigue tests were carried out using plain specimens with a 15-mm gauge length in order to calibrate the cyclic plastic strain range ($\Delta\varepsilon_p$) with the cyclic stress range ($\Delta\sigma$) using hysteresis loops at $N = N_f/2$. The values of $\Delta\varepsilon_p$ in the stress-controlled fatigue tests were determined by using the calibration given by:

$$\Delta\sigma = 1.07 \times 10^3 \Delta\varepsilon^{0.18} \text{ (MPa)} \tag{19}$$

In order to investigate the loss of fracture ductility during the low-cycle fatigue progress, tensile tests on fatigued specimens were performed by interrupting the fatigue tests at several stages up to final fracture. The surface length of the main crack was measured by a plastic replica technique. The effect of small surface cracks on the loss of fracture ductility was studied by comparing the ductilities of fatigued specimens with specimens whose surface layers containing cracks had been removed. Low cycle fatigue tests on specimens containing a drilled hole were also carried out. These specimens need fewer cycles to produce a crack with the same length as plain specimens. Accordingly, the difference in ductility loss in both types of specimen helps one to elucidate critical factors. In particular the difference between the loss in fracture ductility due to the existence of small surface cracks and the loss due to cyclic plastic deformation will be revealed. A push–pull test machine of a closed-loop type was used and the fatigue test frequency was kept in the range 0.05–0.08 Hz. In the tensile fracture tests, the machine cross-head speed was set at 5 mm/min.

### 3.3. Results and discussion

#### 3.3.1. Changes in mechanical properties due to reversals of plastic strain

The monotonic stress–strain curve of a virgin specimen and the cyclic stress–strain curve of the material are shown in Fig. 15. The cyclic stress–strain curve was obtained from the strain-controlled low-cycle fatigue tests at $N=N_f/2$, using another series of smooth specimens with a 15 mm gauge length of 8-mm diameter. These two curves show that the annealed 70/30 brass is a cyclic strain hardening material. It will be shown that the loss of fracture ductility during low-cycle fatigue is not caused by cyclic strain hardening.

Fig. 16 shows the relationship between the relative number of cycles ($N/N_f$) and the ultimate tensile strength ($\sigma_B$) in tensile tests carried out by interrupting fatigue tests at various intermediate cycles $N$ up to $N_f$. The values of the ordinate are the non-dimensional ultimate tensile strength ($\sigma_B/\sigma_{B0}$). The term $l$ in Fig. 16 indicates the length of the main crack in a specimen before the tensile test, and this figure shows that the ultimate tensile strength is barely influenced by the repetitions of the plastic strain range ($\Delta\varepsilon_p$) over the range 0.01–0.025 almost until $N/N_f=1.0$ and that the small surface cracks do not affect ultimate tensile strength. These results should be noted in order to separate the main cause of any loss of fracture ductility from other changes in mechanical properties during low-cycle fatigue.

#### 3.3.2. The main cause of ductility loss due to plastic strain cycling

The residual fracture ductility in low-cycle fatigue decreases with increasing number of cycles ($N/N_{f0}$). Although the cause of this phenomenon is unclear, the view that the change in fracture ductility has a direct correlation with fatigue damage has been predominant in the literature. This view seems to be based on the concept that ductility loss is caused by the loss of strength quality.

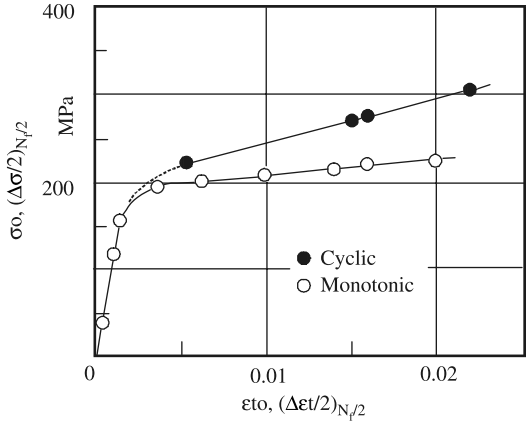


Fig. 15. Comparison between cyclic stress–strain curve and monotonic stress–strain curve.

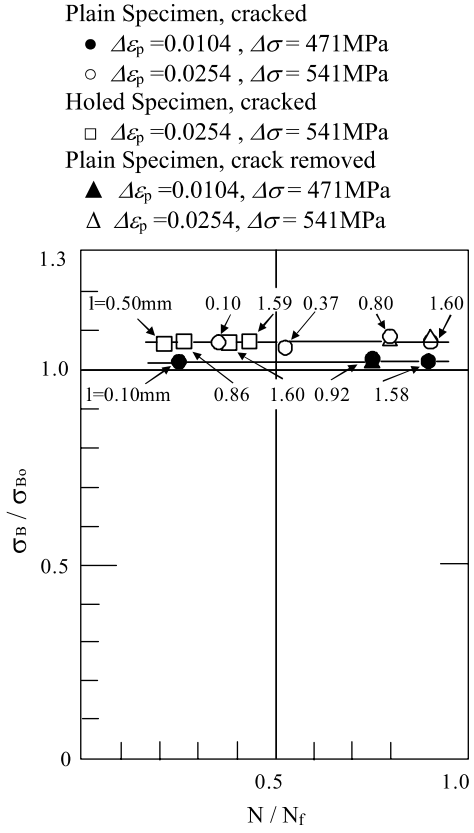


Fig. 16. Relationship between relative number of cycles ($N/N_f$) and ultimate tensile strength $\sigma_B$.

However, according to several studies, [9–11,20,28–30], it is fairly clear that the physical reality of low cycle fatigue damage is the creation of small surface cracks. Therefore, the correlation between the existence of small cracks and ductility loss must be investigated. The key for a complete understanding of fatigue damage is to reveal the mechanism for the loss of fracture ductility due to cracks which, from their size, do not appear to cause this loss.

The relationship between fracture ductility ($\varepsilon_f$) and the increasing number of cycles ($N/N_{f0}$) in 70/30 brass is indicated in Fig. 17, where $N_{f0}$ is the number of cycles to failure of plain specimens. The relationship between the surface length ($l$) of a main crack and $N/N_{f0}$ is shown by Curve A in Fig. 18. In order to measure $\varepsilon_f$ of a fatigued specimen with no crack, the specimen surface was removed by machine turning and thereafter by electro-polishing. The depth of the surface layer removed by turning depended on crack length $l$. The removal of cracks was confirmed by optical microscopy after electro-polishing. At this stage, a tensile test to fracture was performed. The results are indicated by Curve B in Fig. 17, although the values of ductility ($\varepsilon_f$) are a little lower than the initial ductility ($\varepsilon_{f0}$), it can be concluded from a comparison of Curves A and B that the main cause of ductility loss in Curve A is attributable to the existence of small cracks at the surface layer of fatigued specimens. Curves A and B in Fig. 17 branch at $N/N_f=0.6$.

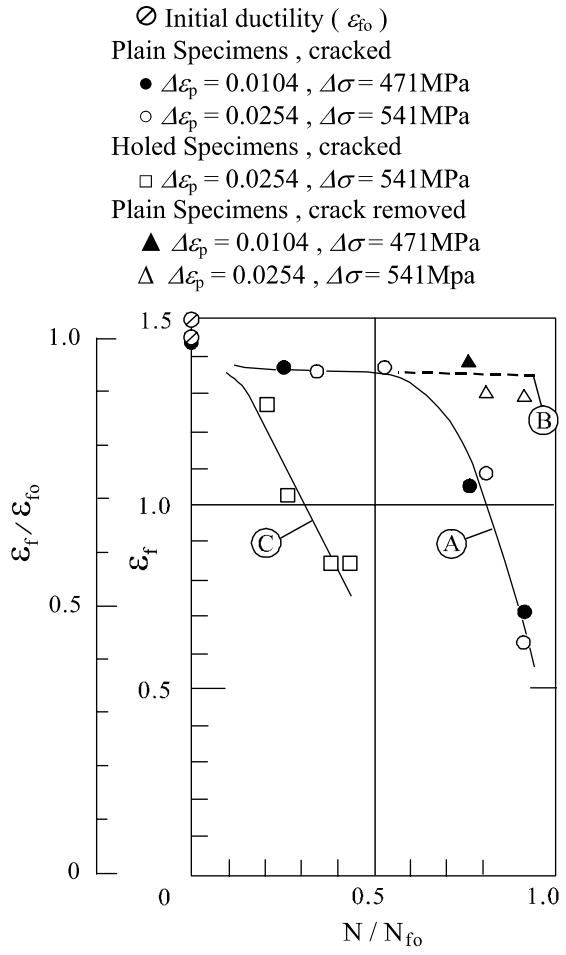


Fig. 17. Relationship between relative number of cycles ($N/N_{f0}$) and fracture ductility $\varepsilon_f$. $N$, number of cycles; $N_{f0}$, number of cycles to failure of plain specimens.

The length of the crack at this point is approximately 400 μm (Fig. 18).

The crack growth curve of a specimen containing a 200-μm diameter hole is shown by Curve C in Fig. 18. Holed specimens need fewer cycles to produce a crack of the same length (including the hole diameter) compared to plain specimens. Curve C in Fig. 17 indicates the results obtained from tensile tests on holed specimens with a crack length of (i) 0.8 mm ($N/N_{f0}=0.26$), (ii) 1.6 mm ($N/N_{f0}=0.4$), and (iii) 0.5 mm ($N/N_{f0}=0.2$). Curve A indicates the results for plain specimens. Here it should be noted that the abscissa in Figs. 17 and 18 is the relative number of cycles ($N/N_{f0}$) of plain specimens. It should be also noted that the decrease in values of Curves A and C for $l=0.5$ and 1.6 mm are regardless of the value of $N/N_{f0}$. Therefore, it can be concluded by comparison of Curve A with Curve C in Fig. 17 that the cause of the loss of fracture ductility is not due to a change in bulk material quality but rather the existence of small surface cracks. This conclusion can be confirmed by choosing crack lengths on the abscissa as shown in Fig. 19. There is no apparent difference between Curves A and C from the viewpoint of ductility. The slight difference between

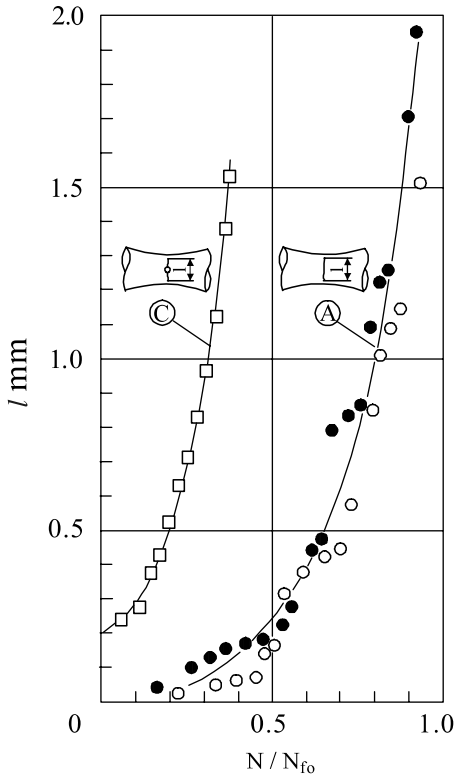


Fig. 18. Crack length ($l$) versus relative number of cycles ($N/N_{f0}$). $N$, number of cycles. $N_{f0}$, number of cycles to failure to plain specimens.

curves A and C at $l=1.6$ mm may be due to the existence of not only a main crack, but other smaller cracks in the case of plain specimens (Curve A). On the other hand, for the case of a holed specimen (Curve C) a main crack emanates from the artificial hole ($d=200$ μm), and other cracks are insignificant in comparison with the main crack and so they hardly affect fracture ductility. If we consider these data (Figs. 17–19) and limit our discussion only to plain specimens, the residual fracture ductility may be used as an insensitive measure of fatigue damage. However, it must be recognised that low cycle fatigue damage is the existence of fatigue cracks on the specimen surface.

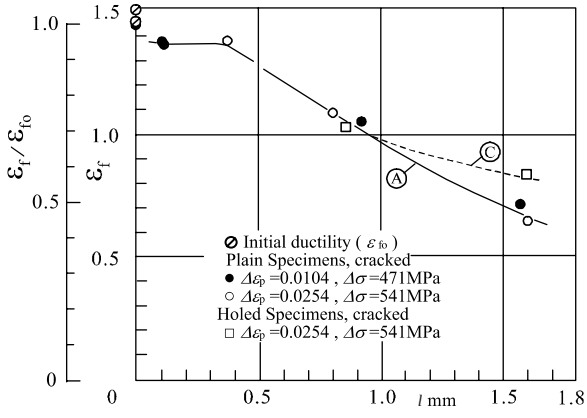


Fig. 19. Crack length ($l$) versus fracture ductility $\varepsilon_f$.

*3.3.3. Morphology of the tensile fracture surface*

The critical crack length that affects the fracture ductility of 70/30 brass is about 400 μm (Figs. 17 and 19). Since the critical crack is too small to be seen by the unaided eye, it is very difficult to predict that such a small crack will cause a loss of fracture ductility for an 8-mm diameter specimen. The loss of fracture ductility by small cracks will be discussed in this section.

Fig. 20 shows the fracture surfaces of tensile tests on plain specimens before and after fatigue tests. In Fig. 20,

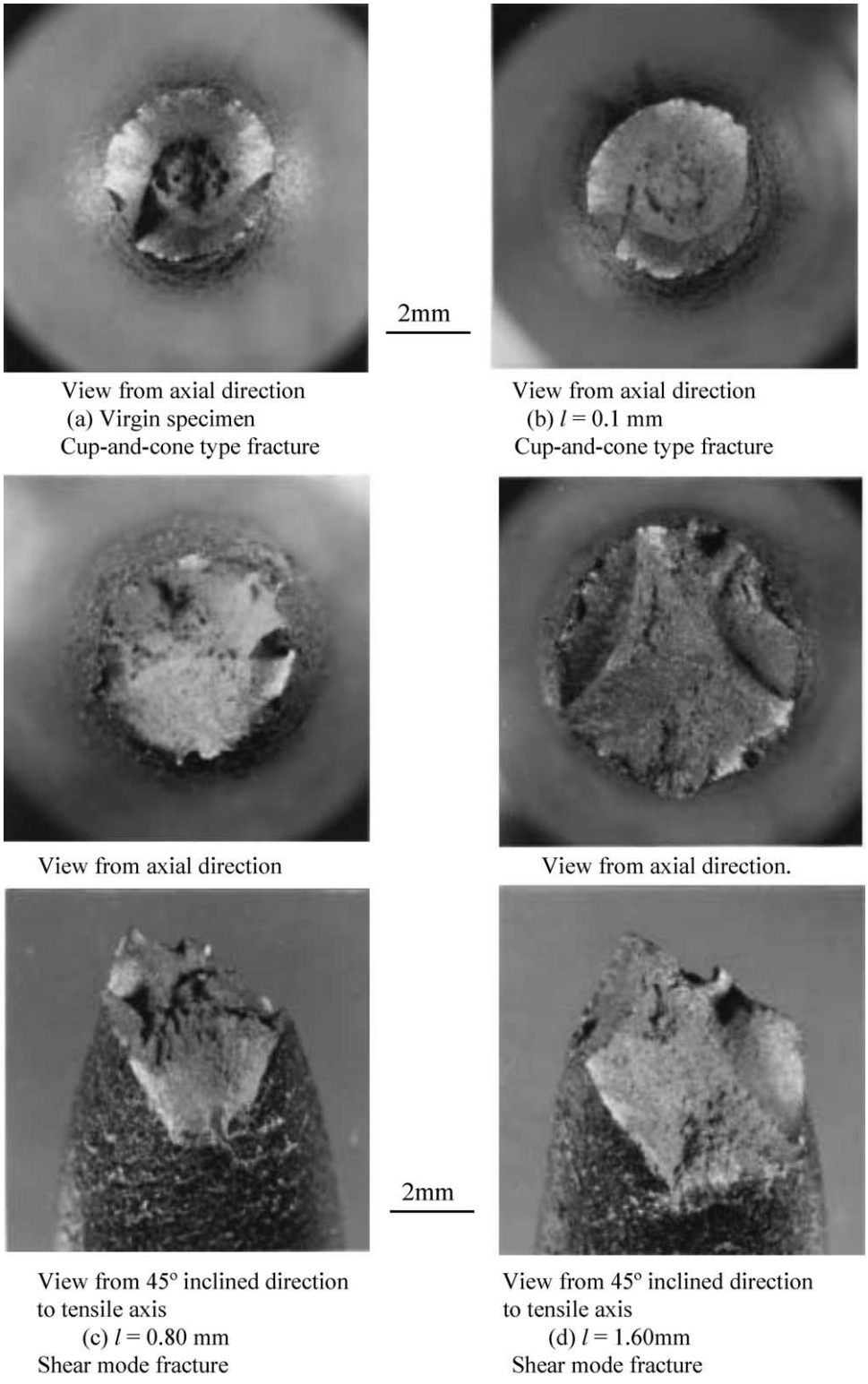


View from axial direction
(a) Virgin specimen
Cup-and-cone type fracture

View from axial direction
(b) $l = 0.1$ mm
Cup-and-cone type fracture

View from axial direction

View from axial direction.

View from 45° inclined direction to tensile axis
(c) $l = 0.80$ mm
Shear mode fracture

View from 45° inclined direction to tensile axis
(d) $l = 1.60$mm
Shear mode fracture

Fig. 20. Cup-and-cone fracture and shear mode fracture in plain specimens ($\Delta\varepsilon_p = 0.0254$).

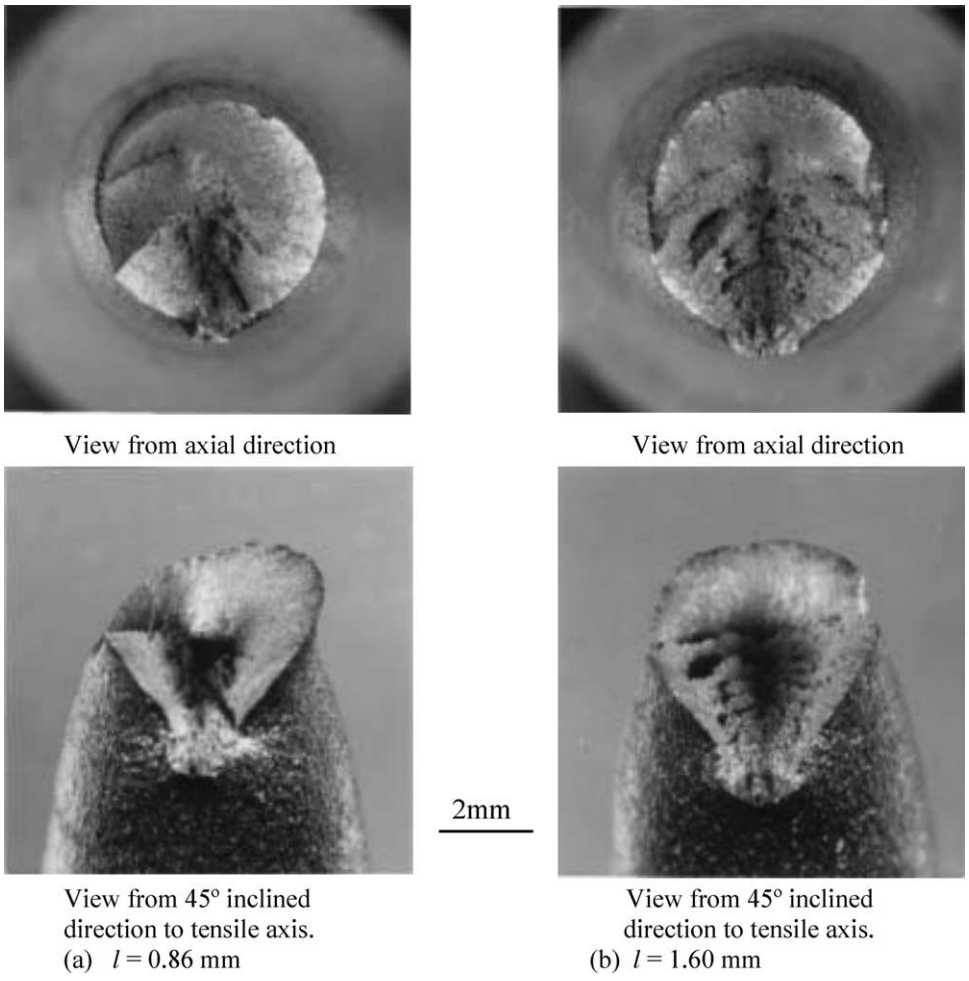


Fig. 21. Shear mode fracture in holed specimens ($\Delta\varepsilon_p = 0.0254$).

part (a) shows the fracture surface with no prior fatigue crack ($N/N_{f0} = 0$), part (b) shows the surface for $l = 0.10$ mm ($N/N_{f0} = 0.35$), (c) shows the surface for $l = 0.80$ mm ($N/N_{f0} = 0.80$), and finally, (d) shows the fracture surface for $l = 1.60$ mm ($N/N_{f0} = 0.90$), where $l$ is the surface length of the dominant fatigue crack before tensile testing. The clear difference between (a), (b), (c) and (d) is that (a) and (b) show the so-called cup-and-cone type fracture and (c) and (d) show an overall shear mode fracture. Since (c) and (d) correspond to the data which show a considerable decrease in fracture ductility (Figs. 17 and 19), we can say that the shear mode fracture is caused by the existence of small cracks in the specimen surface.

Fig. 21 shows the fracture surfaces of holed specimens with a small crack. The length ($l$) of the main fatigue crack shown in Fig. 21(a) and (b) are approximately equal to that of the plain specimens shown in Fig. 20(c) and (d) respectively. Since, in Fig. 21(a) and (b) a single main crack is seen to control the mode of overall tensile fracture behaviour, the features of the shear mode fracture are clearer than those of Fig. 20(c) and (d). These characteristics of the fracture mode lead one to conclude that the loss of fracture ductility is mainly caused by the overall shear mode failure process.

Although it may be difficult to appreciate that the loss of fracture ductility in low-cycle fatigue is controlled by very small surface cracks, the experimental evidence presented in this study clearly reveals the crucial role of a small crack. This behaviour is not only useful in understanding fatigue damage but will also be helpful when discussing the mechanisms of ductile fracture in various materials.

## 4. Conclusions

In order to investigate the correlations between the Coffin-Manson relation, the Palmgren-Miner rule and microcrack initiation and propagation, low-cycle fatigue tests were carried out using plain specimens and holed specimens; the latter containing a very small drilled hole with a diameter of 40, or 100, or 200 μm. The loss of fracture ductility during the low-cycle fatigue process was investigated from the viewpoint of the existence of small surface cracks. The relationship between the growth of

small cracks and the residual fracture ductility during the low-cycle fatigue of 70/30 brass was investigated. The crucial cause for the loss of fracture ductility was elucidated on the basis of microscopic observations. The results are summarised as follows:

1. The low-cycle fatigue process in an annealed medium carbon steel (0.46% C steel) was almost 100% dominated by the growth process of a single crack. In an extreme case, microcrack initiation was observed on the surface of a plain specimen during the first stress cycle.
2. Prior fatigue history virtually has no effect on fatigue damage and hardly influences the subsequent microcrack growth rate.
3. The loss of fracture ductility during low-cycle fatigue was investigated from the viewpoint of the existence of small surface cracks rather than the historical concept of so-called fatigue damage. Should the surface layer of a fatigued specimen be removed by machine-turning and then electro-polishing, in order to remove the surface cracks, the phenomenon of loss of fracture ductility disappears. In the case of plain specimens, the loss of fracture ductility becomes apparent only after the relative number of cycles ($N/N_{f0}$) exceeds 0.6. On the other hand, in the case of holed specimens, the critical number of cycles ($N/N_{f0}$) has lower values than those of plain specimens. From these experimental results, it can be stated that the cause of the loss of fracture ductility during low-cycle fatigue is due to the existence of small surface cracks.
4. The critical length $l$(c) of the crack that causes the loss of fracture ductility is about 400 μm for 70/30 brass. When $l < l$(c), the tensile fracture mode is of the so-called cup-and-cone type. However, when $l > l$(c), the fracture mode changes to a catastrophic shear fracture that starts from small surface cracks. The existence of the critical surface crack length $l$(c) that causes a loss of fracture ductility is important, both for low-cycle fatigue studies, and other aspects of ductile fracture investigations.

## References


[1] Forsyth PJE. A two-stage process of fatigue crack growth. Proceeding of crack propagation symposium, Cranfield, UK; 1961. p. 76–94.
[2] Coffin Jr LF. A study of the effects of cyclic thermal stresses on a ductile metal. Trans ASME 1954;76:931–50.
[3] Manson SS. Behaviour of materials under thermal stress. NACA TN 2933, 1953; and NACA TR 1170; 1954.
[4] Tomkins B. Fatigue crack propagation—an analysis. Philos Mag 1968;18 p. 1041–66.
[5] Boettner RC, Laird C, McEvily AJ. Trans Met Soc AIME 1965;233: 379–87.
[6] Liu HW. Analysis of fatigue crack propagation. NASA CR-2032; 1972.
[7] Frost NE, Dixon JR. Int J Fract Mech 1967;3:301–16.
[8] Morrow JD. Cyclic plastic strain energy and fatigue of metals. ASTM STP 378; 1964. p. 45–87.
[9] Kikukawa M, Ohji K, Okubo N, Yokoi T, Morikawa. Damage and recovery from it in low cycle fatigue. Trans Jpn Soc Mech Eng 1972; 38(305):8–15.
[10] Nisitani H, Morita N. Fatigue damage in low cycle fatigue of carbon steel specimen. Trans Jpn Soc Mech Eng 1973;39(322):1711–9.
[11] Murakami Y, Harada S, Endo T, Tani-ishi H, Fukushima Y. Correlations among growth law of small cracks, low-cycle fatigue law and applicability of Miner's rule. Eng Fract Mech 1983;18(5): 909–24.
[12] Miller KJ. A historical perspective of the important parameter of metal fatigue; and problems for the next century. In: Wu XR, Wang ZG, editors. Proceedings of the seventh international fatigue congress. Fatigue'99, Beijing. Higher Education Press EMAS; 1999. p. 15–39.
[13] Miller KJ, Mohamed HJ, de los Rios ER. Fatigue damage accumulation above and below the fatigue limit. In: The behaviour of short fatigue cracks. EGF (ESIS) Publication No. 1. London: Mechanical Engineering Publications; 1986. p. 491–511.
[14] Weiss V. Analysis of crack propagation in strain-cycling fatigue. In: Fatigue—an interdisciplinary approach Syracuse University Press; 1964. p. 179.
[15] Palmgren A. Die Lebensdauer von Kugellager. Zeitschrift des V.D.I. 68;1924. p. 339–41.
[16] Miner MA. Cumulative damage in fatigue. J Appl Mech 1954;12: A159–A64.
[17] Kikukawa M, Ohji K, Kamata T, Jono M. Low cycle fatigue under varying strain conditions. J Jpn Soc Mech Eng 1967;70(585):1495.
[18] Dowling NE. Fatigue failure predictions for complicated stress–strain histories. J Mater 1972;7(1):71–87.
[19] Endo T, Mitsunaga K, Kobayashi K, Matsuishi M. Damage evaluation of metals for random or varying loading—Three aspects of rain flow method, vol. 1. Proceedings of 1974 symposium on mechanical behavior of materials, 21–24 August 1974. The Society of Materials Science, Japan;1974. p. 371.
[20] Yamada T, Hoshide T, Fujimura T, Manabe M. Preprint Jpn Soc Mech Eng 1982;820(2):138.
[21] Feltner E, Beardmore P. Strengthening mechanism in fatigue. ASTM STP 467; 1970. p. 77.
[22] Feltner E, Laird C. Cyclic stress–strain response of FCC metals and alloys—I: phenomenological experiment. Acta Metall 1967;15: 1621–32.
[23] Feltner E, Laird C. Cyclic stress–strain response of FCC metals and alloys—II: dislocation structures and mechanism. Acta Metall 1967; 15:1633–53.
[24] Coffin Jr LF. Design aspects of high-temperature fatigue with particular reference to thermal stresses. Trans ASME 1956;78:527.
[25] Ohji K. J Jpn Soc Mech Eng 1967;70:36–47.
[26] Duyi Y, Zhenlin W. A new approach to low-cycle fatigue damage based on exhaustion of static toughness and dissipation of cyclic plastic strain energy. Int J Fatigue 2001;23(8):679–87.
[27] Sessler JG, Weiss V. J Basic Eng Trans ASME 1963;85:539–47.
[28] Ohtani N, Abe T, Shimizu M, Kunio T. Trans Jpn Soc Mech Eng 45A 1979;1304–11.
[29] Murakami Y, Makabe C, Nisitani H. Effects of small surface cracks on ductility loss in low cycle fatigue of 70/30 brass. J Test Eval 1989; 17(1):20–7.
[30] Miller KJ, Ibrahim MFE. Damage accumulation during initiation and short crack growth regimes. Fatigue Eng Mater Struct 1981;4:263–77.